A Method to Compute the Interaction Force during Imposed Motions

Gabriel Baud-Bovy
University of Minnesota, Department of Neuroscience
baudb001@tc.umn.edu

Abstract

We present a method to compute the interaction force during an imposed movement. First, we show how to incorporate a kinematic constraint into the equation of motion of a simple but realistic model of the arm. Second, we apply this method to predict the interaction force during an imposed movement of the arm. The results of these simulations are compared to the interaction force recorded when a robot moved the hand of blindfolded subjects according to a predetermined trajectory. The most salient characteristics of the interaction force could be reproduced by assuming that the subjects supported the weight of their arm without attempting to anticipate or resist the imposed movement.

1. Introduction

While the subject of compliant motion has generated a huge literature in robotics [1,2], remarkably little is known about how humans control their movements when they must comply with an external constraint. In addition, most of the studies with human subjects dealt only with passive external constraints such as a rigid surface [3]. For example, McIntyre et al. [4] examined whether subjects monitored the force through sensory feedback or relied on the compliant properties of the arm to slide a hand along a rigid surface. In contrast, our study focuses on the interaction force arising during an *imposed* movement of the arm. Such movements occur when two humans shake hands together or when robots are used in the rehabilitation of stroke patients [5].

The interaction force in such a situation depends on three factors at least: the kinematic characteristics of the imposed motion, the mechanical properties of the arm, and the activity of the subject (e.g. reflex or voluntary contraction of the muscles anticipating or resisting the imposed motion). The main objective of this paper is to describe a method to assess the relative importance of these factors in the interaction force.

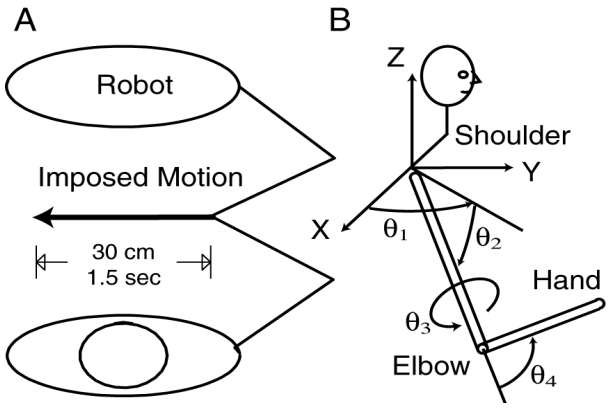

In the Methods, we show how to incorporate a kinematic constraint on the hand position into the equation of motion of a simple but realistic model of the arm to predict the interaction force during an imposed movement. We also describe a procedure to correct errors during the integration which may cause the simulations to diverge from the constraint over a long period of time. In the Results, we apply this method to predict the interaction force under two different hypotheses about the activity of the subjects during an imposed motion. The results of these simulations are compared to the interaction force recorded while a robot moved the hand of blindfolded subjects (Fig. 1A). Finally, we briefly discuss what these preliminary results suggest about the activity of the subjects in this task.

2. Methods

The Arm Model. The arm was modeled as two connected cylindric bodies (Fig. 1B). The first body (upper arm) was connected to the torso by a spherical joint (shoulder) with three degrees of freedom (elbow azimuth, elbow elevation and humeral rotation). The second body (forearm) was connected to the first one by a hinge (elbow) joint with one degree of freedom (elbow flexion).

Install Equation Editor and double-click here to view equation.

The equation of the motion of the arm model is:

where $\theta = [\theta_1\ \theta_2\ \theta_3\ \theta_4]^T$, $\dot{\theta} = [\dot{\theta}_1\ \dot{\theta}_2\ \dot{\theta}_3\ \dot{\theta}_4]^T$ and $\ddot{\theta} = [\ddot{\theta}_1\ \ddot{\theta}_2\ \ddot{\theta}_3\ \ddot{\theta}_4]^T$ are the joint angles, joint velocities and joint accelerations, respectively. Terms on the left side of the equation define the torques acting on the system: $G(\theta)$ is the four dimensional

Install Equation Editor and double-click here to view equation.

Install Equation Editor and double-click here to view equation.

vector of torques defining the effect of gravity at the joints, $L(\theta,\dot{\theta},t)$ is a 4x1 vector of torques defining the force applied by the robot to the hand to keep it on the predefined trajectory, and $F(\theta,\dot{\theta},t)$ is the 4x1 vector defining all other torques acting at the joints. The last term includes the friction and elastic torques resulting from the viscoelastic properties of muscle, as well as the active torques (i.e. those due to reflex and voluntary muscle contractions). This term must be specified to test specific hypotheses about how the arm is controlled during the locating phase. The terms on the right side of the equation describe the torques related to the motion of the system: $M(\theta)$ is the 4x4 inertia tensor (or mass matrix), $B(\theta)$ is the 4x6 matrix of Coriolis coefficients ($\dot{\theta}\dot{\theta}$ = $[\dot{\theta}_1\dot{\theta}_2\ \dot{\theta}_1\dot{\theta}_3\ \dot{\theta}_1\dot{\theta}_4\ \dot{\theta}_2\dot{\theta}_3\ \dot{\theta}_2\dot{\theta}_4\ \dot{\theta}_3\dot{\theta}_4]^T$), $C(\theta)$ is the 4x4 matrix of centripetal coefficients ($\dot{\theta}^2$ = $[\dot{\theta}_1^2\ \dot{\theta}_2^2\ \dot{\theta}_3^2\ \dot{\theta}_4^2]^T$). The Coriolis and centripetal terms must be added to the equation because the frames of reference associated with the coordinates (joint angles) used in the model are not

Install Equation Editor and double-click here to view equation.

Newtonian. Explicit expressions for these matrices can be computed with standard methods [6]. Because they are cumbersome, we do not report them here, but they may be obtained from the author upon request.

The joint angles θ must satisfy the functional endpoint constraint:

where $P(\theta(t))$ is the hand position as a function of the joint angles and $T(t)$ is the hand position imposed by the robot. Because the constraint holds for all values of t, it holds also for all derivatives of $T(t)$. The first time derivative of the constraint is:

where $J(\theta)$ is the 3 by 4 Jacobian matrix:

Computing the second derivative of the constraint yields:

where

Install Equation Editor and double-click here to view equation.

Numerical integration. To integrate equation (14), we used an algorithm described in [8] which is an implementation with step size control and dense output of an

Install Equation Editor and double-click here to view equation.

explicit Runge-Kutta method of order 5. Because rounding errors may lead the solution to diverge from the constraint,

Install Equation Editor and double-click here to view equation.

we also followed a stabilizing strategy which consisted in projecting the joint angles and velocities obtained at each

Install Equation Editor and double-click here to view equation.

and $H_x(\theta)$, $H_y(\theta)$ and $H_z(\theta)$ are the Hessian matrices:

Install Equation Editor and double-click here to view equation.

The equation of motion together with the above constraint defines a differential-algebraic problem [7]. This problem can be solved by using the constraint to calculate the value of the unknown term $L(\theta,\dot{\theta},t)$ in the equation of motion. First, the equation of motion is rewritten as:

Install Equation Editor and double-click here to view equation.

where $Q(\theta,\dot{\theta})$ is the four dimensional vector:

Install Equation Editor and double-click here to view equation.

and $L(\theta,\dot{\theta},t)$ is the vector of torques defined by:

Install Equation Editor and double-click here to view equation.

where $J^T(\theta)$ is the transpose of the Jacobian matrix and $\lambda(\theta,\dot{\theta},t)$ is a three dimensional vector representing the unknown force that the robot must exert to maintain the hand on the predetermined trajectory (see later). Then, the value of $\lambda(\theta,\dot{\theta},t)$ can be found by solving equation (8) for $\ddot{\theta}$:

Install Equation Editor and double-click here to view equation.

Substituting this expression in equation (5) (i.e., the second time derivative of the constraint) yields:

Install Equation Editor and double-click here to view equation.

If the 3 by 3 matrix $J(\theta)M^{-1}(\theta)J^T(\theta)$ is invertible, $\lambda(\theta,\dot{\theta},t)$ can be computed:

Install Equation Editor and double-click here to view equation.

and substituted into equation (10) to yield an ordinary second order differential equation:

Install Equation Editor and double-click here to view equation.

integration step onto the subspace defined by the constraint [7].

Let us assume that the joint angles θ_0 at the end of an integration step do not satisfy the constraint. The problem is to find another set of joint angles θ that minimizes the distance:

(the matrix $M(\theta_0)$ is not necessary but it modifies the norm in a way that makes sense in this context) under the same endpoint constraint:

By differentiating equation (15) with respect to θ and using the method of Lagrange's multipliers, we obtain the following $F(\theta,\mu)$ system of equations:

Because the forward kinematics operator $P(\theta)$ is nonlinear,

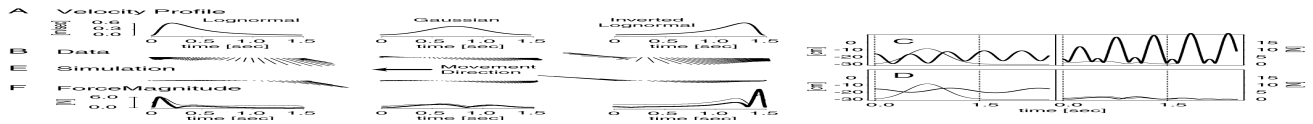

Install Equation Editor and double-click here to view equation.

Install Equation Editor and double-click here to view equation.

the system cannot be solved directly. The solution can be found by using Newtons's iterative method, by repeating the following two steps. In the first step, the following linear system is solved using a standard method (e.g. LU decomposition with back-substitution):

where $\nabla F(\theta_k,\mu_k)$ is the gradient of $F(\theta,\mu)$. In the second step, the new values for the joint angles and Lagrange multipliers are found by computing

Install Equation Editor and double-click here to view equation.

If the initial values $[d\theta_0,d\mu_0]$ are not too far away from the

Install Equation Editor and double-click here to view equation.

solution, the method converges rapidly (the number of iterations was set to ten with initial values $[d\theta_0,d\mu_0] = [\theta_0,0]$).

The joint angle velocities are dealt with in a similar fashion. Let θ be the new joint angles computed above, and let $\_0$ be the joint angle velocities obtained at the end of an integration step. Then the problem is to find the joint angle velocities that minimize:

while satisfying the first time-derivative of the constraint:

The following system is obtained by differentiating equation (20) with respect to $\_$ and using again Lagrange's multipliers method:

This system is linear in respect with $\_$ and μ:

and can be easily solved by standard methods.

The interaction force. Finally, we show that the three-dimensional vector $\lambda(\theta,\_,t)$ has a straightforward interpretation in terms of the interaction force. In vectorial notation, the work is the dot product between the force and displacement vectors. Because the work (energy) required to maintain the hand on the trajectory must be the same when computed in different coordinate systems [6], we have:

where δx is an infinitesimal displacement of the hand in space, $\delta\theta$ is the corresponding displacement in joint space, F is the force applied by the robot to the hand, and $\tau = L(\theta,\_,t) = J^T(\theta)\lambda(\theta,\_,t)$ is the torque component added to the equation

Install Equation Editor and double-click here to view equation.

of motion to account for the endpoint constraint (equation 10). By definition, the Jacobian $J = \delta x/\delta\theta$ relates joint velocity to and cartesian velocity. Thus, substituting $\delta x = J\,\delta\theta$ and $\tau = J^T(\theta)\lambda(\theta,\_,t)$ in equation (24) and simplifying yields:

where J^T is the pseudo-inverse of the transpose of the Jacobian. Thus, $\lambda(\theta,\_,t)$ is the force applied by the robot to the hand to maintain it on the predefined trajectory and, by Newton's Third Law, $-\lambda(\theta,\_,t)$ is the force applied by the hand to the extremity of the robotic arm.

Experimental procedure. We recorded the interaction force for ten blindfolded subjects while a robot (MANUTEC R15, Siemens) moved their hand laterally, from the right to the left (Figure 1.A). These data were recorded as a part of a series of experiments on pointing movements toward kinesthetic targets [9]. Subjects were instructed to let the robot guide their hand to some position in space which they

Install Equation Editor and double-click here to view equation.

Install Equation Editor and double-click here to view equation.

should memorize. The velocity profile of the imposed motion was either lognormal, gaussian or inverted lognormal (Figure 2.A). All movements lasted 1.5 s and were 30-cm long. The interaction force was recorded by a six degrees of freedom force transducer (Mini 40, ATI) mounted below the handle grasped by the subjects at the extremity of the high impedance robotic arm.

3. Results

In this section, we briefly show the results of some simulations and compare them to experimental data. Figure 2.B shows the interaction force for each velocity profile, averaged across participants. The magnitude and orientation of the interaction force varied considerably during the movement. For the lognormal velocity profile, the magnitude of the force was maximum at the beginning of the movement while the opposite was true for the inverted lognormal velocity profile. Force variations during the movement are less obvious for the gaussian velocity profile, partly because their magnitude is small. The shoulder and elbow positions were not recorded. Thus, the comparison between simulated behavior and data will concern mainly the interaction force.

In the simulations, the length, diameter and mass of the two cylinders modeling the upper- and forearm were 30 cm,

4cm, 1.43 kg and 34cm, 3 cm, and 1.32 kg respectively. The initial hand position was 40 cm in front of and 25 cm below the shoulder. In the first set of simulations, we assumed no other forces than those directly related to the inertial properties of the arm. Thus, we set

Install Equation Editor and double-click here to view equation.

in Equation (3). The left panel of Figure 2.C shows the time course of the predicted elbow height (thick line), and of the hand velocity (thin line) in the gaussian velocity profile condition. The right panel contrasts the predicted (thick line) and actual (thin line) magnitude of the interaction force. The simulation was extended to 2.5 s to visualize the behavior of where K_g = 1.565 Nm/rad. The value of K_g did not change throughout the movement and was adjusted so that the elbow would not depart from its initial position if the hand remained immobile at the center of the workspace. This elastic force may be thought of as a very simple model of the deltoid muscle. Figure 2.D shows that the simulations were much more satisfactory. Although some residual oscillations of the elbow remained because the system was not dampened, the predicted force matched the actual force much better. Figure 2.E shows that the predicted interaction forces for the three velocity profiles are remarkably similar to the data (compare with Figure 2.B). Finally, Figure 2.F compares the time course of the magnitude of the predicted and actual interaction force. The actual vs. predicted peaks of the force magnitude were 5.4 vs.6.1 N, 2.0 vs 2.4 N, and 7.2 vs. 10.2 N for the lognormal, gaussian and inverted lognormal velocity profiles respectively. For both asymmetric profiles, the timing of the large peak of force was well predicted (the coefficients of correlation between the time-courses of the actual and predicted force magnitudes were .87, .77, and .92 for the lognormal, gaussian and inverted lognormal velocity profile respectively).

4. Discussion

In summary, we presented a method to predict the interaction force when the hand is constrained to follow a predetermined trajectory with a specific velocity profile. This mathematical tool was used to analyze the actual dynamic behavior of the arm when the hand was moved by a robot.

We were able to reproduce the most salient features of the interaction force by assuming that an upward elastic torque supported the weight of the arm throughout the movement. Like the equilibrium point [10] and the virtual target hypotheses [11, 12], this scheme emphasizes the role of the muscles' elastic properties in addition to the inertial properties of the arm. Because the definition of this force makes no reference to either the final or current position of the hand, these results suggest that the subjects did not try to anticipate the displacements of the hand

The magnitude of the interaction force was smallest when the imposed motion most resembled natural movements (gaussian velocity profile). However, such an observation cannot be interpreted as evidence that the subjects responded differently to natural vs unnatural stimuli since the predicted force magnitude paralleled the actual force.

Although the fit was not perfect, these preliminary results clearly validate the use of bio-mechanical models of the arm to analyze the interaction force recorded during imposed motions. Future work with a larger set of stimuli might be necessary to assess whether more complex models should be considered.

the arm after the end of the movement. Under the sole influence of gravity, the elbow swung like a pendulum even after the end of the movement because there was no damping in the system. The oscillations in the interaction force reflect the swinging motion of the elbow.

Because this behavior is totally unrealistic, we assumed in the next set of simulations that the subjects actively supported the weight of their arm to counteract the effect of gravity. The parametrization of the joint angles in our model afforded a simple way of adding an elastic force to keep the elbow elevated:

Install Equation Editor and double-click here to view equation.

Acknowledgments

This study was completed as a part of the doctoral dissertation [9] of the author under the direction of Prof. Paolo Viviani. I would also like to thank Prof. Ernst Hairer for his help with the mathematical aspects of this study.

References

[1] Chiaverini S, Siciliano B, Villani L. A survey of robot interaction control schemes with experimental comparison. *IEEE/ASME Trans Mechatronics*, 43(2):273-285, 1999.

[2] Zeng GW, Hemami A. An overview of robot force control. *Robotica*, 15(5):473-482, 1997.

[3] Desmurget M, Prablanc C, Jordan M, Jeannerod, M. Are reaching movements planned to be straight and invariant in the extrinsic space? Kinematic comparison between compliant and unconstraint motions. *Quat J Exp Pyschol. A, Hum Exp Psychol*, 52(4):981-1020, 1999.

[4] McIntyre J, Gurfinkel EV, Lipshits MI, Droulez J, Gurfinkel VS. Measurements of human force control during a constrained arm motion using a force actuated joystick. *J Neurophysiol*, 73(3):1201-22, 1995.

[5] Aisen M, Krebs I, Hogan N, McDowell F, Volpe T. The effect of robot-assisted therapy and rehabilitative training on motor recovery following stroke. *Archive of Neurology*, 54, 443-

446, 1997.

[6] Craig JJ. *Introduction to Robotics, 2nd Edition.* Reading, MA:Addison-Wesley, 1986.

[7] Hairer E, Wanner G. *Solving Differential Equations - II. Stiff and differential-algebraic problems, 2nd Edition*. Springer series in Computational Mathematics, Heidelberg, Germany:Springer-Verlag, 1996.

[8] Hairer E, Norsett SP, Wanner G. *Solving Differential Equations - II. Non-stiff problems*. Springer series in Computational Mathematics, Heidelberg, Germany: Springer-Verlag, 1993.

[9] Baud-Bovy G. Pointing toward kinesthetic targets. Thesis 266, Faculty of Psychology and Educational Science, University of Geneva, unpublished doctoral dissertation, 1999.

[10] Feldman AG. Functional tuning of the nervous system with control of movement or maintenance of a steady posture. II. Controllable parameters of the muscle. *Biophys* 11:565-578, 1966.

[11] Flash T. The control of hand equilibrium trajectories in multi-joint arm movements. *Biol Cybern* 57:257-274, 1987.

[12] Gomi H, Kawato M. Equilibrium-point control hypothesis examined by measured arm stiffness during multi-joint movement. *Science*, 272(32-33):117-120, 1996.